GEOPHYSICS, VOL. 56, NO. 2 (FEBRUARY 1991); P. 231–241, 3 FIGS.

Absorbing boundary conditions for elastic waves

R. L. Higdon*

ABSTRACT

Absorbing boundary conditions are needed for computing numerical models of wave motions in unbounded spatial domains. The boundary conditions developed here for elastic waves are generalizations of ones developed earlier for acoustic waves. These conditions are based on compositions of simple first-order differential operators. The formulas can be applied without modification to problems in both two and three dimensions. The boundary conditions are stable for all values of the ratio of *P*-wave velocity to *S*-wave velocity, and they are effective near a free surface and in a horizontally stratified medium. The boundary conditions are approximated with simple finite-difference equations that use values of the solution only along grid lines perpendicular to the boundary. This property facilitates implementation, especially near a free surface and at other corners of the computational domain.

INTRODUCTION

This paper describes a class of absorbing boundary conditions for elastic-wave propagation in two and three dimensions. A separate paper (Higdon, 1990) contains a derivation and extensive analysis of these boundary conditions. The goal of the present paper is to summarize the mathematical ideas and give a detailed description of how the boundary conditions can be implemented in practical computations.

In limited-area numerical modeling of wave propagation in the earth, it is necessary to introduce artificial computational boundaries to keep computation down to a manageable size. If a wave motion arises entirely within the computational domain and if there are no mechanisms beyond the computational boundary to cause significant reflection back toward the computational domain, then the solution near the boundary consists of outgoing wave motions. One then needs boundary conditions that simulate the outward radiation of energy. The homogeneous Dirichlet boundary condition, in which the displacements are held equal to zero, is unsuitable for this purpose; when that boundary condition is used, substantial reflections are generated at the boundary, and the presence of the reflected waves then degrades the interior solution. Instead, one would like to use "absorbing" boundary conditions, for which little reflection is generated.

Several other authors have addressed this problem. A standard absorbing boundary condition is the second-order condition derived by Clayton and Engquist (1977) for elastic-wave calculations involving two dimensions. This boundary condition is based on a paraxial approximation to the elastic-wave equation. Reynolds (1978) developed some absorbing boundary conditions for the acoustic-wave equation and suggested extensions to the elastic case. Liao et al. (1984) developed a boundary extrapolation scheme for acoustic and elastic waves that is closely related to the space-time extrapolation method discussed by various authors (e.g., Higdon, 1986). The extrapolation method of Liao et al. samples the wave field at points not on the computational grid, so an interpolation scheme is required to implement this method. Scandrett et al. (1986) used a first-order boundary condition to absorb Rayleigh waves near a free surface of an elastic medium; this boundary condition fits into the form described below in equation (6), with $m = 1$, $\beta_1 = 1$, and c_P replaced by the speed of Rayleigh waves. Cerjan et al. (1985) and Sochacki et al. (1987) developed methods based on enlarging the computational domain and using a damping mechanism on the additional portion of the domain. Randall (1988) developed a boundary condition based on the following procedure: at each time step, apply a Fourier transform in the tangential space variables, use finite differences to convert the transformed displacements to potentials which satisfy the acoustic wave equation, apply the absorbing boundary condition of Lindman (1975) for acoustic waves, and then convert back to displacements in the space-time domain. Randall (1989) subsequently adapted this algorithm to the velocity-stress formulation of the elastic-wave equation. Long and Liow (1990) decompose the wave field into dilatational and rotational strains, use gradients to identify

Manuscript received by the Editor August 5, 1988; revised manuscript received August 9, 1990.
*Department of Mathematics, Oregon State University, Corvallis, OR 97331-4605.

directions of propagation, and then apply a one-way wave equation to each strain.

The boundary conditions developed in the present paper are based on compositions of simple first-order differential operators, each of which gives perfect absorption for outgoing plane waves traveling at certain velocities and/or angles of incidence. If desired, these parameters can be chosen to take advantage of a priori information about the wave motions that approach the boundary, if such information is available. The performance of the boundary conditions is not very sensitive to the choice of parameters.

The numerical implementation of these boundary conditions is facilitated by the following properties. First, the same formulas can be applied without modification to problems in both two and three dimensions. Second, difference approximations to these boundary conditions use values of the solution only at grid points along lines perpendicular to the boundary. This is useful when a boundary condition is applied along a vertical computational boundary near a horizontal free surface and in a horizontally stratified medium. Numerical experiments have shown that the boundary conditions are effective under such circumstances. Another consequence of the one-dimensional (1-D) stencil is that there is no need to develop special formulas to use at corners of rectangular domains. Various other boundary conditions, such as those of Clayton and Engquist and Randall, do not have 1-D finite-difference stencils, and corner conditions are needed in such cases.

Stability is important in the choice of boundary conditions. Emerman and Stephen (1983) reported the results of practical numerical simulations in which the second-order boundary condition of Clayton and Engquist showed unstable behavior when the ratio of P-wave velocity c_P to S-wave velocity c_S was sufficiently large. Mahrer (1986) reported similar behavior with that boundary condition and also with the boundary condition of Reynolds and with certain types of damping used near the boundary of an extended domain. In contrast, some numerical tests and a theoretical stability analysis have shown that a large value of c_P/c_S does not cause instabilities with the boundary conditions developed in the present paper. Also, Randall (1988) reported that his boundary conditions were found experimentally to be stable for large values of c_P/c_S.

DEVELOPMENT OF BOUNDARY CONDITIONS

The boundary conditions described here are generalizations of ones developed for the acoustic-wave equation $u_{tt} = c^2\nabla^2 u$ by Higdon (1986, 1987) and also independently by Keys (1985). I will first summarize some properties of the acoustic boundary conditions and then describe the generalization to elastic waves.

For simplicity, the discussion in this section is concerned with wave motions on the domain $x > 0$, although in practice one would compute solutions only on a bounded domain. A study of wave motions on the half-space $x > 0$ can be regarded as a localized study of wave behavior near a flat portion of the boundary of a bounded domain. The section on difference approximations describes how the formulas in the present section can be modified for other boundary segments or planes; these modifications are minor.

Consider an acoustic-wave motion on the domain $x > 0$ in either two or three dimensions. At the boundary $x = 0$, the acoustic absorbing boundary conditions have the general form

$$\left\{ \prod_{j=1}^{m} \left[(\cos \alpha_j) \frac{\partial}{\partial t} - c \frac{\partial}{\partial x} \right] \right\} u = 0, \tag{1}$$

where $|\alpha_j| < \pi/2$ for all j. The product notation in equation (1) means to multiply the various first-order operators as polynomials in $\partial/\partial t$ and $\partial/\partial x$. In numerical tests, the case $m = 2$ has proven practical. Finite-difference approximations to equation (1) can be obtained in a manner shown later for boundary conditions for elastic waves.

The form of equation (1) provides a general representation of absorbing boundary conditions for the acoustic-wave equation, in a sense that is described in Proposition 9.1 of Higdon (1986). For example, the boundary conditions of Engquist and Majda (1977, 1979) are equivalent to equation (1) with $\alpha_j = 0$ for all j. The boundary conditions of Trefethen and Halpern (1986) are equivalent to equation (1) for various nonzero α_j's. Renaut and Petersen (1989) analyzed discretizations of second-order ($m = 2$) boundary conditions written in Engquist-Majda and Trefethen-Halpern form.

A motivation for the form of equation (1) is the following. Suppose that a plane wave is traveling out of the domain $x > 0$ at angle of incidence α with speed c. In two dimensions, such a wave can be written in the form

$$f[(x, z) \cdot (\cos \alpha, \sin \alpha) + ct] = f(x \cos \alpha + z \sin \alpha + ct), \tag{2}$$

where f is some function and the other spatial coordinate is denoted by z. An analogous formula holds for three dimensions. When an operator of the form

$$(\cos \alpha) \frac{\partial}{\partial t} - c \frac{\partial}{\partial x} \tag{3}$$

is applied to equation (2), the result is zero. The boundary condition (1) is therefore satisfied exactly by any plane wave traveling out of the domain $x > 0$ with speed c at any of the angles $\pm\alpha_j$. (To check this, first apply the operator that annihilates the given wave, and then let the other operators act on zero.) To put it another way, the boundary condition (1) is exactly compatible with outward radiation of energy via plane waves traveling at any of the angles $\pm\alpha_1 \ldots \pm\alpha_m$, and no reflection is generated at the boundary. More generally, for a plane wave traveling outward at an arbitrary angle of incidence θ, the ratio of the amplitudes of the reflected and incident waves is given by the reflection coefficient

$$\prod_{j=1}^{m} \left| \frac{\cos \alpha_j - \cos \theta}{\cos \alpha_j + \cos \theta} \right|.$$

Each of the factors in this product is less than 1 if $|\theta| < \pi/2$, and the factor with index j is quite small if θ is near $\pm\alpha_j$. Reflection of general wave motions can be analyzed by using Fourier analysis to represent such motions as superpositions of plane waves.

The angles α_j can be chosen to take advantage of a priori

information, if available, about directions from which waves are expected to approach the boundary. For example, if waves near normal incidence are of greatest consequence, then use $\alpha_j = 0$ for all j. If a wide range of angles of incidence is present, then it may be advisable to move the α_j's away from zero so as to distribute the roots of the reflection coefficient and thereby yield a broad range of angles over which the reflection coefficient is small. If it is known that the bulk of the wave motion approaches the boundary at large angles of incidence, then the α_j's can be chosen accordingly. In general, an optimal choice of α_j's is problem-dependent, and a universal criterion for the choice of these angles does not exist. However, numerical tests have indicated that the amount of reflection is not overly sensitive to the values of these angles, and in practice it would probably be enough to make some rough guesses for the α_j's and not worry about experimentation or fine-tuning.

An alternate interpretation of the operator (3) points out a property relevant to wave propagation in stratified media. Consider the case of two space dimensions; a similar interpretation applies to 3-D problems. The earlier interpretation of the operator (3) is based on the plane wave (2), which moves out of the domain $x > 0$ with speed c at angle of incidence α. In this wave, each wavefront intersects a line $z =$ constant at a point that moves toward the boundary with speed $c/\cos\alpha$. (This speed is the reciprocal of the ray parameter; see Aki and Richards, 1980.) The operator (3) is a constant multiple of the operator

$$\frac{\partial}{\partial t} - \left(\frac{c}{\cos\alpha}\right)\frac{\partial}{\partial x},$$

and one can then say that the operator (3) is based on the speed of propagation of points of intersection of wavefronts with lines $z =$ constant. In a sense, the operator (3) is based on what can be observed along lines perpendicular to the boundary.

Now suppose that the operator (3) is applied along a boundary $x = 0$ in a medium whose properties vary only in the z-direction. In such a medium, waves are refracted, and a given wave can have different speeds and directions in different layers. However, the ray parameter $\cos\alpha/c$ is preserved upon refraction, by Snell's law. Thus if the operator (3) is perfectly absorbing for a plane wave in any one layer, then it is perfectly absorbing for that wave in any other layer.

We now consider the case of elastic body waves. For problems in two dimensions, let x and z denote the spatial coordinates, and let u and w denote the x and z displacements, respectively. For the domain $x > 0$, a simple first-order boundary condition at the boundary $x = 0$ is

$$\left(\frac{\partial}{\partial t} - c_P\frac{\partial}{\partial x}\right)u = 0$$
$$\left(\frac{\partial}{\partial t} - c_S\frac{\partial}{\partial x}\right)w = 0. \tag{4}$$

This form is based on the observation that for plane waves traveling at normal incidence to the boundary $x = 0$, the x displacement u is the carrier of P-waves, and the z displacement w is the carrier of S-waves. The condition (4) is therefore perfectly absorbing at normal incidence. This boundary condition is the first-order condition of Clayton and Engquist (1977) and Engquist and Majda (1979).

The boundary condition (4) can be generalized immediately to problems in three dimensions. For the domain $x > 0$, apply the formulas in equation (4) at $x = 0$ for u and w; for the y displacement v, impose $(\partial/\partial t - c_S\partial/\partial x)v = 0$.

The above boundary condition is not satisfied exactly by plane waves traveling in directions other than normal incidence. In this case, a purely outgoing wave motion cannot be a solution of the initial-boundary value problem, so reflected waves must be present in the computed solution. This suggests that an improvement of this boundary condition could be desirable. The boundary conditions discussed here give lower reflections and are based on operators obtained by composing first-order factors of the form (3), much like in the case of acoustic waves. Along the boundary, such an operator is applied to each component of displacement; in general, different operators could be applied to different components. A complicating issue is that the formula for the operator (3) involves a wave speed c, and in the case of elastic body waves there are two different wave speeds c_P and c_S. In general, each component of displacement can experience both P-waves and S-waves, so both wave speeds must be taken into account during the construction and analysis of these boundary conditions.

An example of such a boundary condition is obtained by applying the operator

$$\left[(\cos\alpha_P)\frac{\partial}{\partial t} - c_P\frac{\partial}{\partial x}\right]\left[(\cos\alpha_S)\frac{\partial}{\partial t} - c_S\frac{\partial}{\partial x}\right] \tag{5}$$

to each component of displacement. Here α_P and α_S are parameters that could be adjusted to suit the configuration of the particular problem being solved. The first factor in the operator (5) is oriented to P-waves, and it yields perfect absorption for P-waves traveling outward at angle of incidence $\pm\alpha_P$; the second factor is oriented to S-waves and yields perfect absorption for S-waves at angles of incidence $\pm\alpha_S$. A crucial point in the reflection analysis given in Higdon (1990) is that each factor has a very substantial value in helping absorb the other type of wave. The first factor is oriented toward P-waves but helps absorb S-waves; the second is oriented toward S-waves but helps for P-waves. The main idea is that in factors of the form (3), a change in the value of c is equivalent to a change in the value of $\cos\alpha$. If the first factor in expression (5) is multiplied by c_S/c_P, the result can be regarded as an S-wave factor that is perfectly absorbing for S-waves at angles of incidence

$$\pm\cos^{-1}\left(\frac{c_S}{c_P}\cos\alpha_P\right).$$

Such angles might not be optimal for absorbing S-waves, but such a factor definitely helps absorb such waves. Similarly, the second factor in expression (5) can be regarded as a P-wave factor by multiplying by c_P/c_S.

A more general boundary condition can be obtained by applying an operator

$$\prod_{j=1}^{m} \left(\beta_j \frac{\partial}{\partial t} - c_P \frac{\partial}{\partial x} \right) \tag{6}$$

to each component of displacement at the boundary. Here the parameters $\beta_1, \ldots, \beta_m$ are positive dimensionless constants. Up to a multiplicative constant, the operator (5) fits into the general form (6); in that example, $m = 2$, $\beta_1 = \cos \alpha_P$, and $\beta_2 = (c_P/c_S) \cos \alpha_S$. The use of c_P in each factor in expression (6) amounts to a normalization of coefficients, and it is done solely for notational convenience. If each of the β_j's in expression (6) were chosen to be less than or equal to 1, then the boundary condition would be oriented mainly to the absorption of *P*-waves; however, the boundary condition would still provide useful absorption of *S*-waves. If the values of the β_j's were all near c_P/c_S, then the boundary condition would be oriented mainly to *S*-waves. In some numerical computations described below, the second-order version of expression (6) was used with $\beta_1 = 1$ and $\beta_2 = c_P/c_S$, and the third-order version of expression (6) was used with $\beta_1 = 1$, β_2 between 1 and c_P/c_S, and $\beta_3 = c_P/c_S$. Similar values can be recommended for general use. Numerical experiments have indicated that the performance of the operator (6) is not particularly sensitive to small adjustments in the β_j's.

A quantitative description of the performance of (6) is given by the graphs of reflection coefficients plotted in Figure 1. In each plot, the solid curve is the graph of a reflection coefficient corresponding to the second-order version of expression (6) with $\beta_1 = 1$ and $\beta_2 = c_P/c_S$. The value of c_P/c_S affects the reflection coefficient, and in this example it is taken to be $\sqrt{3}$. The dotted curve in each graph corresponds to the third-order version of expression (6) with $\beta_1 = 1$, $\beta_2 = 1.3$, and $\beta_2 = c_P/c_S = \sqrt{3}$. Different values of the β_j's would give different graphs.

Another type of boundary condition could be obtained by applying different operators to different components of displacement. For example, at the boundary $x = 0$ of the domain $x > 0$, one could apply to the x displacement an operator oriented mainly to *P*-waves, and apply to the other components an operator oriented mainly to *S*-waves. In some 2-D numerical tests described in Higdon (1990), this approach did not yield significant changes in performance

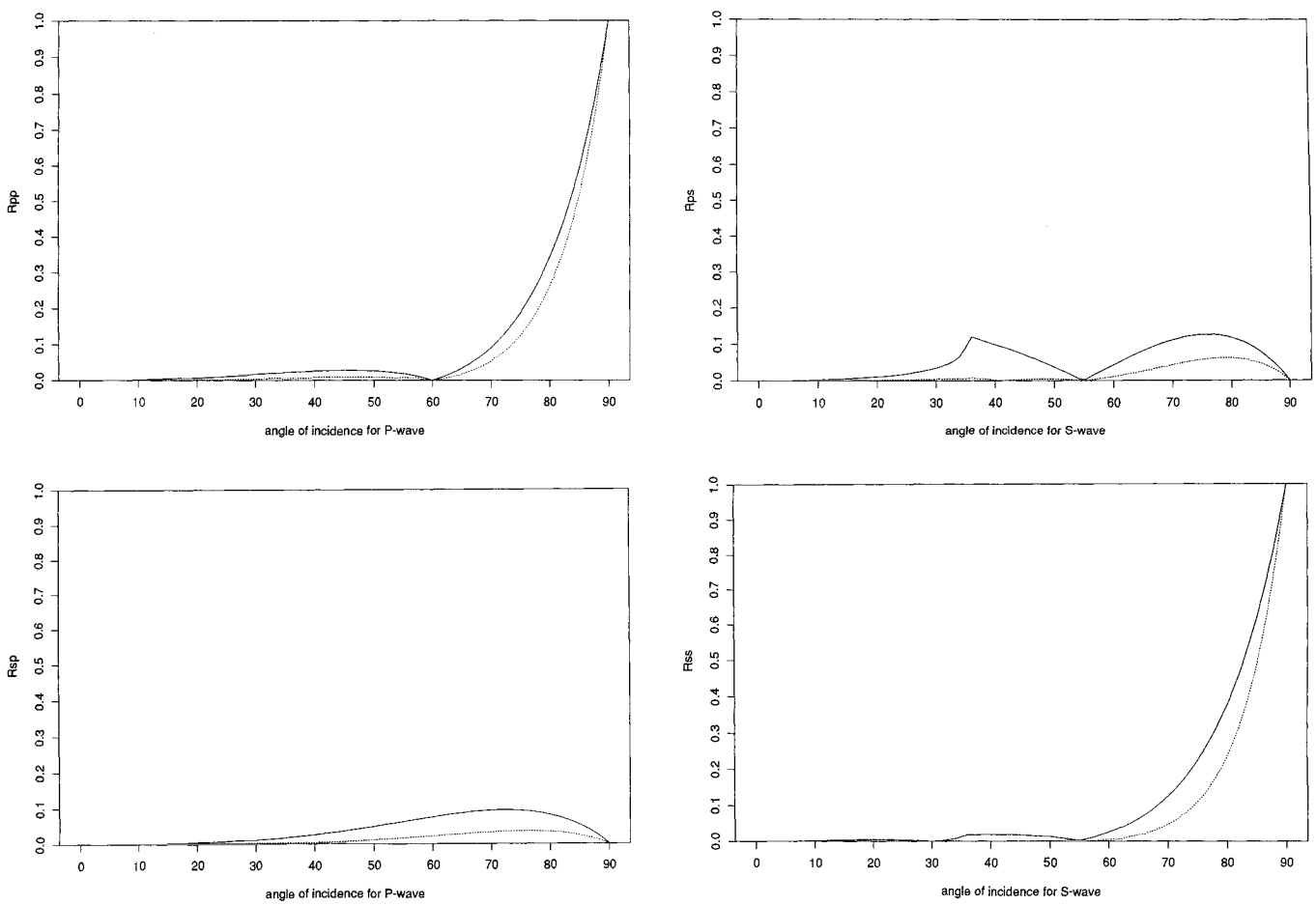

FIG. 1. Graphs of reflection coefficients. In each plot, the solid curve is the graph of a reflection coefficient corresponding to the second-order ($m = 2$) version of the operator (6) with $\beta_1 = 1$ and $\beta_2 = \sqrt{3} = c_P/c_S$; the dotted curve corresponds to the third-order ($m = 3$) version of the operator (6) with $\beta_1 = 1$, $\beta_2 = 1.3$, and $\beta_3 = \sqrt{3} = c_P/c_S$. R_{PP}: amplitude of reflected *P*-wave due to incident *P*-wave of unit amplitude. R_{SP}: reflected *S*-wave due to incident *P*-wave. R_{PS}: reflected *P*-wave due to incident *S*-wave. R_{SS}: reflected *S*-wave due to incident *S*-wave. Each coefficient is plotted as a function of the angle of incidence of the incident wave.

over boundary conditions obtained by using the same operator on all components.

Applying the same operator to all components of displacement leads to major simplifications in the analysis of reflection and stability properties. This is the case analyzed in Higdon (1990). The analysis of stability relies on a stability criterion that is an analogue of one developed by Kreiss (1970) for first-order hyperbolic systems. In this analysis, the value of the velocity ratio c_P/c_S does not play any role, so a large value of c_P/c_S would not induce unstable behavior.

DIFFERENCE APPROXIMATIONS

This section contains derivations of formulas for difference approximations to boundary conditions for rectangular regions in two or three dimensions.

In the interior of the computational domain, the elastic-wave equation can be discretized using centered second-order finite differences. The resulting difference equations for 2-D problems are given by Kelly et al. (1976), and analogous formulas apply to three dimensions. When this approach is used to discretize the interior equation, the interior scheme can be used to compute displacements at all grid points except those on the boundary. The boundary conditions must then be used to obtain the displacements at the boundary points.

First consider boundary conditions for 2-D problems. For this case, suppose the spatial domain is the rectangular region defined by $A < x < B$ and $0 < z < H$. Let Δx, Δz, and Δt denote the step sizes in x, z, and t, respectively; and denote the x and z displacements at the grid points by $u^N_{J,M} = u(A + J\Delta x, M\Delta z, N\Delta t)$ and $w^N_{J,M} = w(A + J\Delta x, M\Delta z, N\Delta t)$. Suppose the interior finite-difference scheme has been used to compute displacements at all interior grid points at time level $N + 1$. It is then necessary to compute boundary values at that time level.

First consider the boundary segment at $x = A$. In this case, for the continuous problem one can use the boundary formulas developed in the preceding section. To derive difference approximations, define shift operators E_x and E_t by

$$E_x u^N_{J,M} = u^N_{J+1,M}$$

and

$$E_t u^N_{J,M} = u^{N+1}_{J,M}.$$

Then $E_x^{-1} u^N_{J,M} = u^N_{J-1,M}$ and $E_t^{-1} u^N_{J,M} = u^{N-1}_{J,M}$. An operator $\beta\partial/\partial t - c_P \partial/\partial x$ can be approximated by

$$D(E_x, E_t^{-1}) = \beta\left(\frac{I - E_t^{-1}}{\Delta t}\right)[(1-b)I + bE_x] - c_P\left(\frac{E_x - I}{\Delta x}\right)\left[(1-b)I + bE_t^{-1}\right], \quad (7)$$

where I is the identity operator and b is a constant. In the first term in equation (7), the factor $(I - E_t^{-1})/\Delta t$ represents a backward time difference, and the factor $[(1 - b)I + bE_x]$ represents a weighted average in x with weighting coefficients $1 - b$ and b. The time differences will be taken with respect to the new time level $N + 1$, so backward time differences are used. The second term in equation (7) represents a forward space difference of a weighted time average. In principle, one could use different pairs of weighting coefficients in the two terms in equation (7); however, the resulting difference operator would be equivalent to an operator of the same form for which the pairs are the same (see Lemma 1 of Higdon, 1987).

Suppose the general boundary operator (6) of order m is applied to each component of displacement at $x = A$. The boundary condition for u can then be discretized by

$$\left[\prod_{j=1}^{m} D_j(E_x, E_t^{-1})\right] u^{N+1}_{0,M} = 0; \quad (8)$$

the same formula is also applied to w. In equation (8), $D_j(E_x, E_t^{-1})$ approximates $\beta_j\partial/\partial t - c_P\partial/\partial x$. In the formula for D_j, one could choose the weighting coefficient b to depend on j; however, this possibility is not likely to be significant in practice and will not be considered here. To implement equation (8), formally multiply the formulas for the D_j's as polynomials in the symbols E_x and E_t^{-1}, and solve for the term that does not contain E_x or E_t^{-1}. That term corresponds to $u^{N+1}_{0,M}$. The other terms correspond to values of u at nearby grid points. For example, $E_x u^{N+1}_{0,M} = u^{N+1}_{1,M}$ and $E_x^2 E_t^{-2} u^{N+1}_{0,M} = u^{N-1}_{2,M}$.

Before the operators $D_j(E_x, E_t^{-1})$ in equation (8) are multiplied together, it is useful to simplify them. A manipulation of equation (7) yields

$$\frac{\Delta t}{(\beta + \nu)(1-b)} D(E_x, E_t^{-1}) = I + q_x E_x + q_t E_t^{-1} + q_{xt} E_x E_t^{-1}, \quad (9)$$

where q_x, q_t, and q_{xt} are scalar constants defined by

$$q_x = \frac{b(\beta + \nu) - \nu}{(\beta + \nu)(1-b)},$$

$$q_t = \frac{b(\beta + \nu) - \beta}{(\beta + \nu)(1-b)}, \quad (10)$$

and

$$q_{xt} = b/(b-1).$$

Here $\nu = c_P\Delta t/\Delta x$. In the boundary condition (8), scalar multiples of the D_j's do not matter, so in practice, one would multiply operators having the form of the right side of equation (9).

In the case $m = 2$, the boundary condition for the continuous problem is obtained by applying the operator

$$\left(\beta_1 \frac{\partial}{\partial t} - c_P \frac{\partial}{\partial x}\right)\left(\beta_2 \frac{\partial}{\partial t} - c_P \frac{\partial}{\partial x}\right) \quad (11)$$

to each component of displacement. The boundary operator (11) is approximated by the discrete operator

$$D_1(E_x, E_t^{-1}) D_2(E_x, E_t^{-1}).$$

Represent D_1 and D_2 in the form of equations (9) and (10), with appropriate β's; in this case, let r_x, r_t, and r_{xt} denote the coefficients of E_x, E_t^{-1}, and $E_x E_t^{-1}$, respectively, in the representation (9) of D_2. The discrete boundary condition for u is then

$$u_{0,M}^{N+1} =$$

$$\gamma_{01} u_{1,M}^{N+1} + \gamma_{02} u_{2,M}^{N+1} + \gamma_{10} u_{0,M}^{N} + \gamma_{11} u_{1,M}^{N} + \gamma_{12} u_{2,M}^{N} + \gamma_{20} u_{0,M}^{N-1} + \gamma_{21} u_{1,M}^{N-1} + \gamma_{22} u_{2,M}^{N-1}, \quad (12)$$

where

$$\begin{aligned} \gamma_{01} &= -(q_x + r_x), \\ \gamma_{02} &= -q_x r_x, \\ \gamma_{10} &= -(q_t + r_t), \\ \gamma_{11} &= -(q_x r_t + q_t r_x + q_{xt} + r_{xt}), \\ \gamma_{12} &= -(q_x r_{xt} + r_x q_{xt}), \\ \gamma_{20} &= -q_t r_t, \\ \gamma_{21} &= -(q_t r_{xt} + r_t q_{xt}), \\ \gamma_{22} &= -q_{xt} r_{xt}. \end{aligned} \quad (13)$$

The same formula as equation (12) is also applied to w; just replace each occurrence of u in equation (12) with w. More generally, if one wanted to apply a different second-order operator of the form of the operator (11) to w, then one would apply the same formula as in equation (12), but with different choices of the parameters β_1 and β_2.

The notation in equations (12) and (13) includes a mechanism for checking for errors in coding. In the term involving γ_{ij} in equation (12), the index i refers to the number of time shifts backward from time level $N + 1$. The index i is also equal to the total number of subscripts t in each individual term in the formula for γ_{ij} in equation (13). The index j plays a similar role regarding x shifts and subscripts x.

Equations (12) and (13) are concerned with second-order boundary conditions ($m = 2$). In a similar manner, higher order boundary conditions ($m > 2$) can be developed to obtain greater absorption, at the cost of additional complexity. Explicit formulas for the case $m = 3$ are given in the Appendix. However, higher order conditions without any undifferentiated terms can be less robust than second-order conditions, in the sense that accidental incompatibilities between initial conditions and boundary conditions are more likely to generate mild instabilities in the computed solution (Higdon, 1990). This is a statement about any boundary condition containing derivatives, not just the ones developed here. For the boundary operator (6), this situation can be relieved by adding positive constants to at least one of the first-order factors of that operator.

Next consider boundary conditions for the boundary segment at $x = B$. For this case, it is necessary to modify the operator (6). For the earlier case, the inward normal direction is the positive x-direction; in the present case, the inward normal direction is the negative x-direction. The reversal of coordinate direction means that the boundary operator is a composition of factors of the form $\beta\partial/\partial t + c_P \partial/\partial x$, which can be discretized by

$$\beta\left(\frac{I - E_t^{-1}}{\Delta t}\right)\left[(1-b)I + bE_x^{-1}\right] + c_P\left(\frac{I - E_x^{-1}}{\Delta x}\right)\left[(1-b)I + bE_t^{-1}\right]. \quad (14)$$

In the second term, a backward space difference is used. The difference operator (14) has the same form as the earlier difference operator (7), except that E_x^{-1} replaces E_x. When operators of the form (14) are multiplied together, the same algebraic steps are performed as were done to obtain equations (9) and (10) and equations (12) and (13), and the final result has the same form as before. The interchange of E_x^{-1} and E_x means that backward space shifts are used instead of forward space shifts. That is, the same formulas are used in both cases, where in each case the spatial shifts are taken in the inward normal direction.

For example, when $m = 2$, one has the following. Suppose that $B = A + L\Delta x$. The boundary condition for u at this boundary segment is

$$u_{L,M}^{N+1} = \gamma_{01} u_{L-1,M}^{N+1} + \gamma_{02} u_{L-2,M}^{N+1} + \gamma_{10} u_{L,M}^{N} + \gamma_{11} u_{L-1,M}^{N} + \gamma_{12} u_{L-2,M}^{N} + \gamma_{20} u_{L,M}^{N-1} + \gamma_{21} u_{L-1,M}^{N-1} + \gamma_{22} u_{L-2,M}^{N-1}, \quad (15)$$

where the coefficients γ_{ij} are given in equation (13). The boundary condition for w has the same form.

Boundary conditions for the segment $z = H$ are handled similarly.

At a corner of a rectangular domain, the displacements can be obtained by applying the boundary condition on one of the intersecting boundary segments right on up to the corner. Displacements at neighboring points on the other segment should be computed first.

Next, suppose that the boundary at $z = 0$ is a free surface. Along such a boundary, it is necessary to implement the physical boundary conditions of zero (or forced) normal and tangential stresses. The implementation of the free-surface conditions must be coordinated with the implementation of the absorbing boundary conditions along the side boundaries $x = A$ and $x = B$. This process is facilitated by the 1-D stencil of the discrete absorbing boundary conditions described here.

A method of implementing the zero-stress conditions at a free surface was described by Vidale and Clayton (1986). Let n denote the number of grid points at $z = 0$ between the side boundaries, not including the corner points at $x = A$ and $x = B$. Vidale and Clayton developed a simultaneous system of $2n$ linear equations that needs to be solved at each time step. Each equation is obtained from a centered difference approximation to a stress at one of the grid locations between $x = A$ and $x = B$. However, the unknowns in the system are the displacements at the grid points along the free surface, including those at the corners, so the number of unknown quantities is $2n + 4$. The number of unknowns in the linear system can be reduced to the number of equations by modifying the Vidale-Clayton method as follows. The absorbing boundary conditions described here have a 1-D stencil, so each displacement at each corner point can be

written in terms of displacements at grid points at $z = 0$ *between* the side boundaries. The corner displacements are thereby eliminated from the linear system, and the number of equations equals the number of unknowns. This procedure requires minor modifications of the coefficient matrices derived by Vidale and Clayton. Once the linear system is solved, the corner displacements are calculated explicitly from the displacements at $z = 0$ just obtained.

Similar remarks apply to implementation in a stratified medium. In some numerical computations described later, wave motions were computed in a stratified medium consisting of homogeneous layers separated by parallel horizontal interfaces. This homogeneous formulation was used instead of the heterogeneous elastic wave equation because the computational model included strong discontinuities of velocities across the interfaces. At each interface, it was necessary to implement the physical interface conditions of continuity of stresses and displacements. This was done as follows. At each interface, introduce an extra horizontal row of grid points, so that the lower two grid rows of the upper layer refer to the same positions in space as the upper two grid rows of the lower layer. For each layer, formulate centered finite difference approximations to each stress and equate stresses between the two layers. In the upper medium, use the elastic-wave equation to calculate displacements at all grid points except those on the lowermost grid row; in the lower medium, calculate displacements everywhere except on the uppermost grid row. On one of the grid rows that remains (either one is all right; the choice is arbitrary), assign displacements by using the fact that the displacements at those positions in space were computed during the computation for the other layer. For the remaining grid row, compute displacements by solving a linear system obtained from the equations for stresses. This is similar to what is done at the free surface. Again, the formulation of the linear system is facilitated by the 1-D stencil of the absorbing boundary conditions along the vertical computational boundary.

The difference formulas derived in this section can also be applied to 3-D problems. Suppose that the computational domain is the region defined by $A < x < B$, $C < y < D$, and $0 < z < H$. Operators of the form of equation (6) would be applied to each component of displacement at each boundary plane. At the boundary $x = A$, formulas (12) and (13) would be used when $m = 2$; the only change needed is to modify the notation to include an index for the additional space variable y. Similar remarks apply to the other boundary planes and to the corners of the region.

NUMERICAL RESULTS

This section describes two series of numerical computations involving the boundary conditions defined by the operator (6). Each series of tests involved two dimensions. In the first series, the boundary conditions were compared with the second-order boundary condition of Clayton and Engquist (1977) for the case of a homogeneous medium. In the second set of computations, wave motions were computed in a heterogeneous medium consisting of homogeneous layers separated by horizontal interfaces. The computational model includes a free surface, large velocity contrasts between layers, and a large value of c_P/c_S in two layers.

In the first series of computations, boundary conditions were tested at the boundary $x = 0$ for the domain $x > 0$. Dimensionless space and time coordinates were used, with $c_P = 1$. In the graphics given here, the performance of boundary conditions is illustrated on the domain Ω defined by $0 < x < 1$, $-1 < z < 1$. (For notational convenience, the z-coordinate was chosen to be centered about $z = 0$. In this case, z is not literally a measure of depth.) Solutions were actually computed on a larger subdomain of the half-space $x > 0$; in the time interval on which solutions were computed, the only boundary effects seen here are due to the boundary at $x = 0$. Some additional related computations were performed to test the behavior of the operator (6) near a corner of the computational domain, and the corner strategy described in the preceding section was verified as effective.

Two different sets of initial data were tested, one that yielded a symmetrically expanding P-wave and another that yielded a symmetrically expanding S-wave. In each case there was a broad range of angles of incidence. The two cases yielded similar conclusions, so only the P-wave computations are described here.

The expanding P-wave was centered about the point $(x, z) = (.5, 0)$ and was based on the amplitude profile

$$f(r) = \begin{cases} \varepsilon \sin^3 [\pi(r - r_1)/(r_2 - r_1)], & r_1 < r < r_2 \\ 0, & \text{otherwise,} \end{cases}$$

where $r = [(x - .5)^2 + z^2]^{1/2}$, $r_1 = .17$, $r_2 = .42$, and ε is a constant. The P-wave was obtained by requiring $(u, w) = f(r)\ [(x - .5)/r,\ z/r]$ at $t = 0$ and expanding the profile outward by distance $c_P \Delta t$ to obtain the solution at time $t = \Delta t$. Here $\Delta x = \Delta z = 1/96$, and $c_P \Delta t/\Delta x = 0.80$.

The second-order centered finite-difference approximation to the elastic-wave equation (Kelly et al., 1976) was used in the interior. In discrete boundary operators of the form of equation (7), the weighting coefficient b was taken to be 0.40. Some experiments showed that positive values of b gave slightly better performance than $b = 0$, but the amount of reflection was not very sensitive to the choice of b. Optimal values of b are likely problem dependent.

The amount of reflection was identified by comparing the computed solutions with a reflectionless solution obtained by computing on a larger domain extending into the half-space $x < 0$. Measurements of reflections were based on calculating the quantity

$$\left[(u - U)^2 + (w - W)^2\right]^{1/2} \tag{16}$$

at each grid point in Ω, for fixed t. Here (u, w) is the solution computed with a boundary, and (U, W) is the reflectionless solution obtained by computing on the larger region. In the graphics given here, the quantity (16) is expressed as a percentage of the maximum amplitude of displacement in the initial data.

Figure 2 shows contour plots of this percentage reflection, as a function of (x, z), at the dimensionless time $t = 0.7$. At this value of t, the wave crest contacts the boundary $x = 0$ at an angle of incidence approximately equal to 63 degrees. In

these tests the velocity ratio is $c_P/c_S = \sqrt{3}$. For each boundary condition, the maximum amplitude of reflection varies with time, and the maximum amplitudes at $t = 0.7$ are given in the captions of Figures 2a–2c. The overall results obtained using the second-order version of the operator (6) and the second-order condition of Clayton and Engquist are roughly comparable; the Clayton-Engquist condition is a little more effective near normal incidence and a little less effective near tangential incidence. The third-order version of the operator (6) yields lower reflections than either of the second-order conditions. Different choices of β_j's in the operator (6) would give somewhat different reflection patterns in Figures 2a and 2b.

Additional computations were performed with larger values of c_P/c_S; such values are typical of less rigid materials. For the second-order Clayton-Engquist condition, unstable behavior was apparent for $c_P/c_S = 2.6$, 2.8, and 3.0, with the strength of the instability increasing as c_P/c_S increased. For $c_P/c_S = 3.0$, no instabilities were observed with the second- and third-order versions of the operator (6) and various choices of β_j's.

The second series of computations illustrates the behavior of the boundary condition (6) in a layered medium with a free surface. Again, dimensionless space and time coordinates were used. This model includes strong velocity contrasts between layers, and $c_P/c_S = 10.0$ in two of the layers. As described near the end of the section on difference approximations, the homogeneous elastic-wave equation was used in each layer, and interface conditions were imposed between layers. The results of the computations are shown in Figure 3.

In this case, $\Delta x = \Delta z = 1/80$, and $\Delta t = 1/100$. Waves were generated by a forcing term in the normal stress condition that was a constant multiple of

$$\cos^2 [\pi(x - 1)/2L] \cos^2 [\pi(t - T - \Delta t)/2T]$$

for $|x - 1| \le L$ and $|t - T - \Delta t| \le T$. The forcing was zero for all other (x, t). Here, $L = 4\Delta x$ and $T = 15\Delta t$, and the durations of the pulse in x and t were $2L$ and $2T$, respectively.

For the computation illustrated in Figure 3b, the second-order version of the operator (6) was applied to each component of displacement along the side and bottom boundaries, with $\beta_1 = 1$, $\beta_2 = \sqrt{3}$, and $c_P = 1$. The same parameters in the operator (6) were used in all layers, even

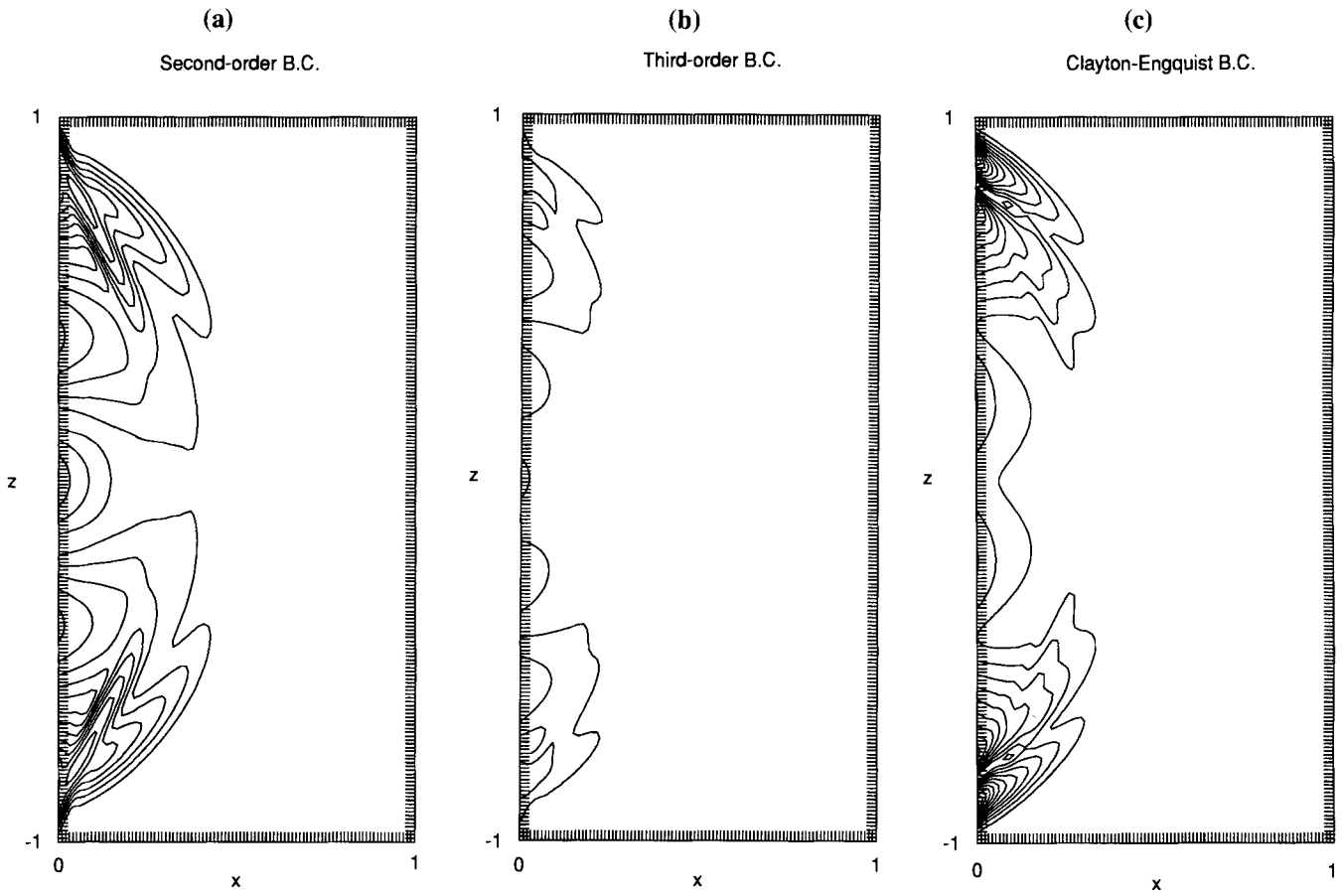

FIG. 2. Comparison of boundary conditions in a homogeneous medium. A symmetrically expanding P-wave encounters the left boundary, and various absorbing boundary conditions are applied at that boundary. The graphs are contour plots of the amount of reflection at the dimensionless time $t = 0.7$. In each case, the amount of reflection is given as a percentage of the maximum amplitude of displacement in the initial data, with contour interval equal to 0.5 percent. (a) Second-order ($m = 2$) version of the operator (6), with $\beta_1 = 1$ and $\beta_2 = \sqrt{3} = c_P/c_S$. In this plot, the maximum amplitude of reflection is 3.8 percent. (b) Third-order ($m = 3$) version of the operator (6), with $\beta_1 = 1$, $\beta_2 = 1.3$, and $\beta_3 = \sqrt{3} = c_P/c_S$. The maximum amplitude is 1.5 percent. (c) Second-order Clayton-Engquist boundary condition. The maximum amplitude is 6.2 percent.

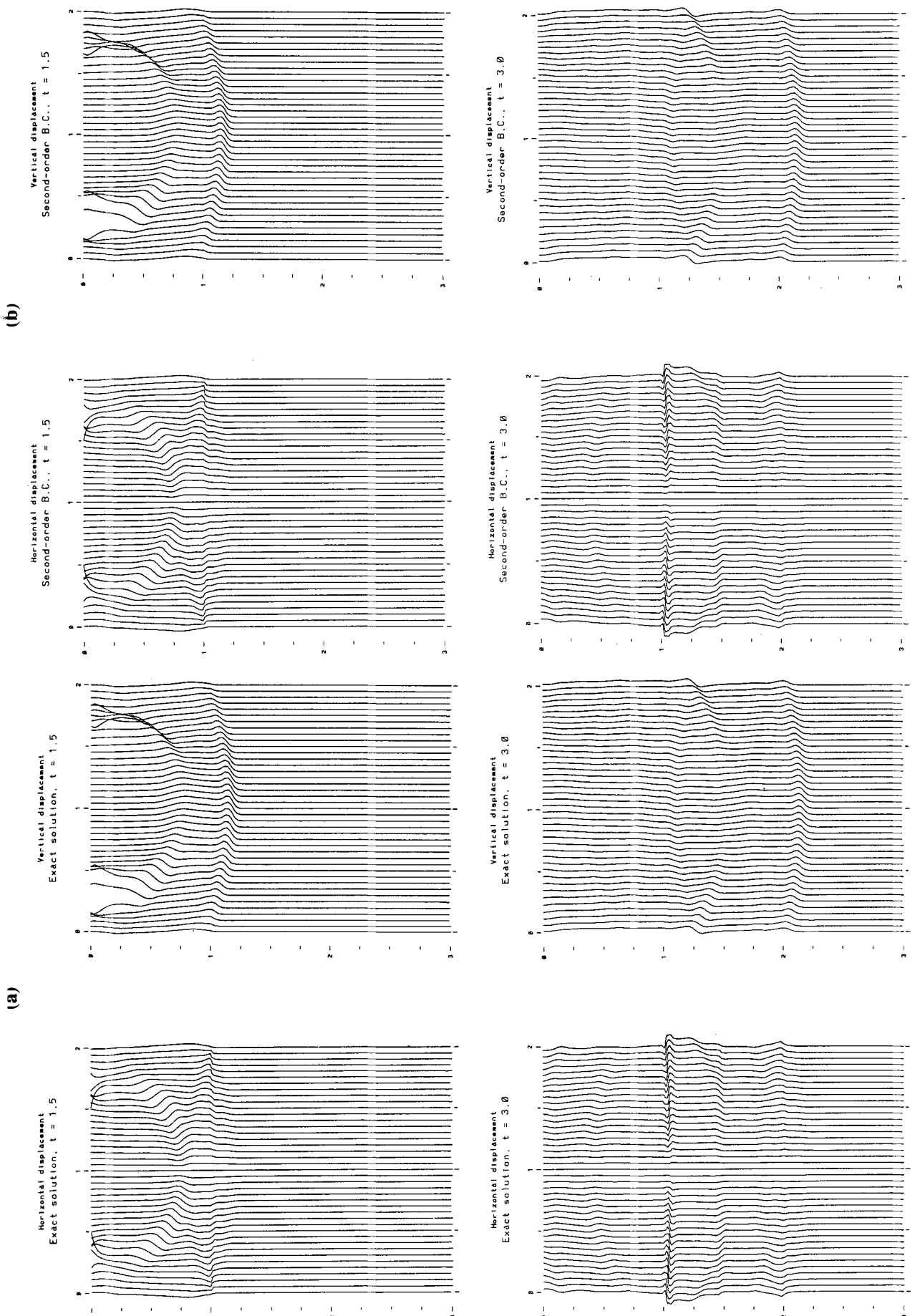

FIG. 3. Performance of boundary conditions in a layered medium. The spatial domain is defined by $0 \le x \le 2$, $0 \le z \le 3$. A free surface is located at $z = 0$, and the medium consists of five homogeneous layers separated by interfaces at $z = 1.0$, $z = 1.5$, $z = 2.0$, and $z = 2.5$. In the top, third, and fifth layers $c_P = 1$ and $c_S = 1/\sqrt{3} = 0.577$. In the other two layers, corresponding to $1.0 < z < 1.5$ and $2.0 < z < 2.5$, the velocities are $c_P = 0.5$ and $c_S = 0.05$. The waves are generated by a forcing term in the normal stress at the free surface. The surface source is located at $x = 1$. (a) Exact (reflectionless) solution obtained by computing on a larger domain. Horizontal displacements are on the left, and vertical displacements are on the right. Displacements are shown at times $t = 1.5$ and $t = 3.0$. (b) Solution obtained by using the second-order ($m = 2$) version of the operator (6) on the side and bottom boundaries. The parameters in the operator (6) are given the same values in all layers.

those for which $c_P \neq 1$. This is in accordance with the remarks made earlier about the operator (3) being based on the ray parameter $(\cos \alpha)/c$, which is invariant under refraction in a stratified medium. The parameters used here yield perfect absorption for P-waves and S-waves traveling at normal incidence in layers for which $c_P = 1$. In the computation illustrated in Figure 3b, the boundary conditions give good absorption for the downgoing P- and S-waves, even though they are not traveling at normal incidence to the computational boundary. The parameters used here are considered generic values, and little attempt was made to tune the boundary condition to the particular wave motions seen in this example. Figure 3 also shows that the surface source used here produced strong Rayleigh waves along the free surface, and these were absorbed effectively at the side boundaries, because the speed of Rayleigh waves is close to c_S.

The solution computed with absorbing boundary conditions and the exact (reflectionless) solution were compared by overlaying computer plots. In the plots shown in Figure 3, the only case that showed visible discrepancies was the horizontal displacement at time $t = 3.0$. The discrepancies are located mainly at an upcoming S-wave near $z = 0$ and at the downgoing S-wave near $z = 1$. The latter wave lies in one of the slow layers; in these layers, S-waves move very slowly and are not resolved well by the grid. (The purpose of these computations is not to resolve S-waves in the slow layers, but instead to subject the boundary conditions to extreme conditions.)

To quantify the difference between the exact solution and the solution computed with absorbing boundary conditions, the amount of reflection at each t was computed by finding the maximum of the quantity (16) over the spatial domain shown, and this reflection was compared to the reflection generated at the same t by the homogeneous Dirichlet boundary condition $u = w = 0$. At time $t = 1.5$, the reflection in Figure 3b is 2.5 percent of that generated by the Dirichlet condition; at time $t = 3.0$, the reflection is 8.6 percent. The third-order version of the operator (6) was also tested, with $\beta_1 = 1$, $\beta_2 = 1.3$, and $\beta_3 = \sqrt{3}$. In this case, the third-order condition gave reflections of 0.6 and 3.0 percent at times $t = 1.5$ and $t = 3.0$, respectively. Computations for longer times showed an increase in the amount of reflection; at time $t = 5.0$, the second-order condition gave a reflection of 21.5 percent and the third-order condition yielded 12.6 percent reflection.

The latter effect was not significant in a related computation for which $c_P/c_S = \sqrt{3}$ in all layers. All other aspects of the computation were the same as the one described above, including the values of c_P. The second-order boundary condition gave reflections of 2.5, 7.1, and 6.0 percent at times $t = 1.5$, $t = 3.0$, and $t = 5.0$, respectively. The third-order condition gave reflections of 0.5, 2.7, and 8.1 percent at the same values of t. Similar results were obtained for a homogeneous medium.

SUMMARY

The boundary conditions developed here are obtained by composing simple first-order differential operators. Each of these operators causes perfect absorption of all outgoing plane waves having a particular value of the ray parameter. For more general wave motions, the amount of artificial reflection is a continuous function of parameters, and the boundary conditions are highly absorbing over a broad range of angles of incidence. The same boundary formulas are valid for problems in both two and three dimensions, and the methodology described here applies to both acoustic waves and elastic waves. The boundary conditions are approximated by relatively simple difference formulas. The boundary conditions are stable for all values of the ratio of P-wave velocity to S-wave velocity, and they are effective near a free surface and in layered media having strong velocity contrasts between layers.

ACKNOWLEDGMENTS

I thank the reviewers for their useful comments.

This material is based upon work supported by the National Science Foundation under grant no. DMS-8802649.

REFERENCES

Aki, K., and Richards, P. G., 1980, Quantitative seismology: Theory and methods, **I** and **II**: W. H. Freeman and Co.

Cerjan, C., Kosloff, D., Kosloff, R., and Reshef, M., 1985, A nonreflecting boundary condition for discrete acoustic and elastic wave equations: Geophysics, **50**, 705–708.

Clayton, R., and Engquist, B., 1977, Absorbing boundary conditions for acoustic and elastic wave equations: Bull. Seis. Soc. Am., **67**, 1529–1540.

Emerman, S. H., and Stephen, R. A., 1983, Comment on "Absorbing boundary conditions for acoustic and elastic wave equations," by R. Clayton and B. Engquist: Bull. Seis. Soc. Am., **73**, 661–665.

Engquist, B., and Majda, A., 1977, Absorbing boundary conditions for the numerical simulation of waves: Math. Comp., **31**, 629–651.

——— 1979, Radiation boundary conditions for acoustic and elastic wave calculations: Comm. Pure. Appl. Math., **32**, 313–357.

Higdon, R. L., 1986, Absorbing boundary conditions for difference approximations to the multi-dimensional wave equation: Math. Comp., **47**, 437–459.

——— 1987, Numerical absorbing boundary conditions for the wave equation: Math. Comp., **49**, 65–90.

——— 1990, Radiation boundary conditions for elastic wave propagation: SIAM J. Numerical Analysis, **27**, 831–870.

Kelly, K. R., Ward, R. W., Treitel, S., and Alford, R. M., 1976, Synthetic seismograms: A finite-difference approach: Geophysics, **41**, 2–27.

Keys, R. G., 1985, Absorbing boundary conditions for acoustic media: Geophysics, **50**, 892–902.

Kreiss, H.-O., 1970, Initial boundary value problems for hyperbolic systems: Comm. Pure Appl. Math., **23**, 277–298.

Liao, Z. P., Wong, H. L., Yang, B. P., and Yuan, Y. F., 1984, A transmitting boundary for transient wave analyses: Scientia Sinica (Series A), **27**, 1063–1076.

Lindman, E. L., 1975, "Free-space" boundary conditions for the time dependent wave equation: J. Comput. Phys., **18**, 66–78.

Long, L. T., and Liow, J. S., 1990, A transparent boundary for finite-difference wave simulation: Geophysics, **55**, 201–208.

Mahrer, K. D., 1986, An empirical study of instability and improvement of absorbing boundary conditions for the elastic wave equation: Geophysics, **51**, 1499–1501.

Randall, C. J., 1988, Absorbing boundary condition for the elastic wave equation: Geophysics, **53**, 611–624.

——— 1989, Absorbing boundary condition for the elastic wave equation: velocity-stress formulation: Geophysics, **54**, 1141–1152.

Renaut, R. A., and Petersen, J., 1989, Stability of wide-angle absorbing boundary conditions for the wave equation: Geophysics, **54**, 1153–1163.

Reynolds, A. C., 1978, Boundary conditions for the numerical solution of wave propagation problems: Geophysics, **43**, 1099–1110.

Scandrett, C. L., Kriegsmann, G. A., and Achenbach, J. D., 1986, Scattering of a pulse by a cavity in an elastic half-space: J. Comput. Phys., **65**, 410–431.

Sochacki, J., Kubichek, R., George, J., Fletcher, W. R., and Smithson, S., 1987, Absorbing boundary conditions and surface waves: Geophysics, **52**, 60–71.

Trefethen, L. N., and Halpern, L., 1986, Well-posedness of one-way wave equations and absorbing boundary conditions: Math. Comp., **47**, 421–435.

Vidale, J. E., and Clayton, R. W., 1986, A stable free-surface boundary condition for two-dimensional elastic finite-difference wave simulation: Geophysics, **51**, 2247–2449.

APPENDIX

THIRD-ORDER BOUNDARY CONDITIONS

This appendix gives explicit formulas for the third-order ($m = 3$) version of the discrete boundary condition (8). For reasons given in the section on difference approximations, third-order conditions may be less robust than second-order conditions. In some situations it might be necessary to add a positive constant to at least one of the difference operators D_j in equation (8), and the formulas in this appendix would then be modified accordingly.

These formulas are stated for a boundary $x = A$ of a computational region for which $x > A$. However, the formulas can be applied immediately to other boundary segments or planes by using the ideas about reversal of coordinate direction described in the section on difference approximations.

In the third-order version of equation (8), represent the difference operators D_1, D_2, and D_3 as scalar multiples of the operators

$$I + q_x E_x + q_t E_t^{-1} + q_{xt} E_x E_t^{-1},$$

$$I + r_x E_x + r_t E_t^{-1} + r_{xt} E_x E_t^{-1}, \text{ and}$$

$$I + s_x E_x + s_t E_t^{-1} + s_{xt} E_x E_t^{-1},$$

respectively. The coefficients q_x, q_t, and q_{xt} are given in equation (10), with $\beta = \beta_1$. The rs and ss are given by the same formulas, but with $\beta = \beta_2$ and $\beta = \beta_3$, respectively. The discrete boundary condition (8) is then equivalent to

$$u_{0,M}^{N+1} = \sum_{i,j} \gamma_{ij} u_{j,M}^{N+1-i},$$

where the sum is taken over all i and j for which $0 \le i \le 3$ and $0 \le j \le 3$, except $i = j = 0$. The coefficients γ_{ij} are given by

$$\gamma_{01} = -(q_x + r_x + s_x),$$

$$\gamma_{02} = -(q_x r_x + r_x s_x + q_x s_x),$$

$$\gamma_{03} = -q_x r_x s_x,$$

$$\gamma_{10} = -(q_t + r_t + s_t),$$

$$\gamma_{11} = -[q_x(r_t + s_t) + r_x(q_t + s_t) + s_x(q_t + r_t) + q_{xt} + r_{xt} + s_{xt})],$$

$$\gamma_{12} = -[q_x r_x s_t + q_x r_t s_x + q_t r_x s_x + q_x(r_{xt} + s_{xt}) + r_x(q_{xt} + s_{xt}) + s_x(q_{xt} + r_{xt})],$$

$$\gamma_{13} = -(q_x r_x s_{xt} + q_x r_{xt} s_x + q_{xt} r_x s_x),$$

$$\gamma_{20} = -(q_t r_t + r_t s_t + q_t s_t),$$

$$\gamma_{21} = -[q_x r_t s_t + q_t r_x s_t + q_t r_t s_x + q_t(r_{xt} + s_{xt}) + r_t(q_{xt} + s_{xt}) + s_t(q_{xt} + r_{xt})],$$

$$\gamma_{22} = -[q_{xt} r_{xt} + q_{xt} s_{xt} + r_{xt} s_{xt} + q_x(r_{xt} s_t + r_t s_{xt}) + r_x(q_{xt} s_t + q_t s_{xt}) + s_x(q_{xt} r_t + q_t r_{xt})],$$

$$\gamma_{23} = -(q_x r_{xt} s_{xt} + q_{xt} r_x s_{xt} + q_{xt} r_{xt} s_x),$$

$$\gamma_{30} = -q_t r_t s_t,$$

$$\gamma_{31} = -(q_t r_t s_{xt} + q_t r_{xt} s_t + q_{xt} r_t s_t),$$

$$\gamma_{32} = -(q_t r_{xt} s_{xt} + q_{xt} r_{xt} s_t + q_{xt} r_t s_{xt}), \text{ and}$$

$$\gamma_{33} = -q_{xt} r_{xt} s_{xt}.$$

Several observations can be used to check for errors in implementing these formulas. If the indicated multiplications are carried out, the formulas contain a total of 63 additive terms. For each γ_{ij}, the first subscript is equal to the number of time steps back from time level $N + 1$, and it is also equal to the total number of subscripts t in each additive term in the formula for γ_{ij}. The second subscript is equal to the number of space steps in the inward normal direction and is also equal to the total number of subscripts x in each term. Each formula is symmetric in q, r, and s.